Met. Mater. Int., Vol. 21, No. 5 (2015), pp. 950~955
doi: 10.1007/s12540-015-5043-0

One-Pot Synthesis of h-BN Fullerenes Usinsg a Graphene Oxide Template

Sang Sub Kim[1], Tran Van Khai[2], Yong Jung Kwon[2], Akash Katoch[1], Ping Wu[3,*], and Hyoun Woo Kim[2,*]

[1]Division of Materials Science and Engineering, Inha University, Incheon 402-751, Korea
[2]Division of Materials Science and Engineering, Hanyang University, Seoul 133-791, Korea
[3]Singapore University of Technology and Design, Singapore 138682, Singapore

(received date: 19 January 2015 / accepted date: 23 May 2015)

Hexagonal-boron nitride (*h*-BN) fullerenes were synthesized from a graphene oxide (GO) template by simultaneously heating the GO and B_2O_3 in the presence of NH_3 gas. Transmission electron microscopy (TEM) observations revealed that a considerable amount of product had a fullerene-like nanostructure. Typical BN fullerenes have a polyhedral shape, being hollow nanocages. Lattice-resolved TEM and X-ray diffraction consistently demonstrated the formation of *h*-BN fullerenes. The FTIR spectrum exhibited absorption bands at approximately 800 and 1378 cm^{-1}, which were related to the *h*-BN structure. The Raman spectra exhibited peaks at 1368 and 1399 cm^{-1}, which can be related to BN sheets and BN fullerenes, respectively. The photoluminescence spectrum of the *h*-BN fullerenes taken at 8 K exhibited intense white-light emission. To reveal the origin of the broad emission band, which could be a superimposition of several peaks, we used a deconvolution procedure based on Gaussian functions. We proposed a growth mechanism of the *h*-BN fullerenes and verified it with a thermodynamic calculation. This work provides a cost-effective approach to synthesize fullerene-type boron nitride on a production scale.

Keywords: semiconductors, fullerenes, chemical synthesis, transmission electron microscopy (TEM), raman spectroscopy

1. INTRODUCTION

Following the discovery of fullerenes, C_{60}, by Kroto *et al*. in 1985 [1], a number of investigations have been performed to understand their electronic and structural properties [2]. Researchers have also tried to identify fullerene-like compounds based on elements other than carbon [3]. One of the most attractive layered-structured materials is boron nitride (BN), an extremely important III-V group compound with a wide band-gap of 5.2 eV at room temperature. Because boron and nitrogen atoms in B-N bonds are isoelectronic to carbon atoms in C-C bonds, BN structures have properties similar to those of their carbon analogs. BN structures also exist in cubic (diamond-like), hexagonal (*h*, graphite-like), turbostratic, and amorphous forms [4]. BN structures are hollow cages similar to fullerenes [4], nanotubes [5], and nanocapsules [6] and are chemically stable, heat resistant, and have semiconducting properties. Cubic BN is one of the hardest known materials. Some properties of BN compounds, however, differ greatly from those of their carbon analogs. For example, BN fullerene-like materials have a wider band gap and higher heat resistance in air than do carbon fullerenes [7].

*Corresponding author: hyounwoo@hanyang.ac.kr, wuping@sutd.edu.sg

BN fullerene-like materials have attracted enormous interest for practical applications as well as scientific research. They are useful in electronic devices, high heat-resistant semiconductors, and insulator lubricants [8]. Similar to carbon nanocapsules, BN fullerene-like materials can encapsulate foreign elements within their hollow cages [9]. BN fullerene-like materials consisting of light-weight elements can store many gas molecules per unit weight [10]. For example, a $B_{36}N_{36}$ cage can store up to 18 hydrogen molecules at 0 K [11,12]. BN has a higher heat resistance than carbon, which is favorable for gas storage [10]. Furthermore, controlling the size, helicity, composition, layer number, and included cluster can modify the electronic, optical, and magnetic properties of B-C-N nanocages [13]. The BN fullerene-like materials with nanoporous channels in a regular, simple cubic lattice are also attractive as molecular sieves or nanomembranes [11].

Despite their technical importance and wide applicability, the nanotube structures of BN fullerene-like materials are energetically less favorable than C fullerenes [3]. Accordingly, obtaining BN fullerene-like materials is difficult [3]. To prepare BN fullerene-like materials, some techniques have been introduced. The first experimental evidence of the formation of small BN cage-like molecules was suggested by means of electron irradiation [14]. Isolated BN

fullerenes with a small number of layers, including single-layer structures, were created by laser ablation [13]. In addition, the arc-melting method has been used to synthesize BN fullerenes [10]. In addition to these high-energy sources, chemical reactions have been used with catalytic templates. Examples include nitriding MgB_2 with NH_4Cl and NH_4Cl-NaN_3 [15], using carbon nanotube (CNT) templates [16], and reacting BBr_3 with synergic nitrogen sources (i.e. $NaNH_2$ and NH_4Cl) [17]. Development of a cost-effective means to synthesize BN fullerenes will facilitate their use.

In the present work, we synthesized *h*-BN fullerenes in one pot by heating a mixture of graphene oxide (GO) and B_2O_3 in the presence of NH_3 gas. This technique is analogous to Han *et al*.'s work, in which CNTs were used as a template [16]. In the present method, GO was a template. The structure, morphology, and bonding nature of the synthesized *h*-BN fullerenes were investigated. In addition, a growth mechanism was proposed based on a thermodynamic calculation. The synthesis method developed in this work will expedite the practical application of BN fullerenes for various functions.

2. EXPERIMENTAL PROCEDURES

In the present study, BN fullerenes were synthesized by continuously heating a mixture of GO and B_2O_3 in an NH_3 atmosphere at 1150 °C. Single- and few-layer GO sheets were synthesized using a modified Hummers' method [18]. The Bi_2O_3 powders were purchased from the Junsei Chemical Co., Ltd. The optical microscopy image reveals that the diameter of Bi_2O_3 powders ranges from 1-50 μm. Subsequently, 5 grams of B_2O_3 was dissolved in 250 ml of ethanol, 0.5 grams of GO was added, and the resulting mixture was sonicated for 5 h. Next, the mixture was heated at around 60 °C and stirred with a magnetic stir bar to remove the ethanol, resulting in a black powder. The powder (300 mg) was placed in an alumina boat, which was placed in an alumina tube and heated at 250 °C for 2 h to remove all the moisture under a flow of NH_3 (25 standard cubic centimeter per minute, sccm) and Ar (100 sccm) gases. The temperature was then increased to 1150 °C over 80 min. The substitution reaction was carried out for 5 h. Next, to further reduce the amount of oxygen remaining in these materials, the temperature was increased to 1500 °C and held for 5 h. After heating, the reaction chamber was cooled to 700 °C, and the NH_3 and Ar gases were turned off. The tube was opened at both ends and held at this temperature for 3 h to oxidize any remaining carbon, resulting in the conversion of the $B_xC_yN_z$ products to BN fullerenes. Finally, the reaction chamber was naturally cooled to room temperature. The original black GO sheets were converted into a white layer of product.

Transmission electron microscopy (TEM) images were taken with a JEOL JEM-2010 transmission electron microscope (JEOL Ltd., Tokyo, Japan; 200 kV). For TEM observations, the products were sonicated in acetone for 2 h and centrifuged at 6000 rpm for 10 min. Subsequently, the suspension was dropped on a carbon holey grid and dried in a vacuum oven at 50 °C for 72 h. An X-ray diffraction (XRD) pattern was acquired using a D/MAX Rint2000 diffractometer model (Rigaku, Tokyo, Japan) with CuKα radiation (λ = 1.54178 Å, 40 kv, 200 mA). Fourier transform infrared (FTIR) spectra (500-4000 cm^{-1}) were acquired with a Nicolet IR100 FTIR spectrometer. Photoluminescence (PL) spectra were obtained at 8 K with a SPEC-1403 PL spectrometer at 325 nm from a He-Cd laser (Kimon, Japan).

3. RESULTS AND DISCUSSION

TEM observations revealed that considerable amounts of product had a fullerene-like nanostructure. Figures 1(a) and 1(b) show TEM images of typical fullerene-like nanostructures. The BN fullerenes, being hollow nanocages, had a polyhedral shape, with relatively sharp corners. Similar corners have been observed in a previous study [10]. Also, smaller fullerenes were observed within/near larger fullerenes (Fig. 1(c)). Figure 1(d) shows that the spacing between the lattice planes of the fullerenes was nearly 0.33 nm, which corresponds to the d_{0002} spacing of hexagonal BN phase (JCPDS card: No. 85-1068). Of the several BN polymorphs, including *h*-BN, rhombohedral BN (*r*-BN), cubic BN (*c*-BN), and wurtzite BN (*w*-BN) [19], *h*-BN has numerous advantages, such as low density, low dielectric constant, high thermal stability, high conduc-

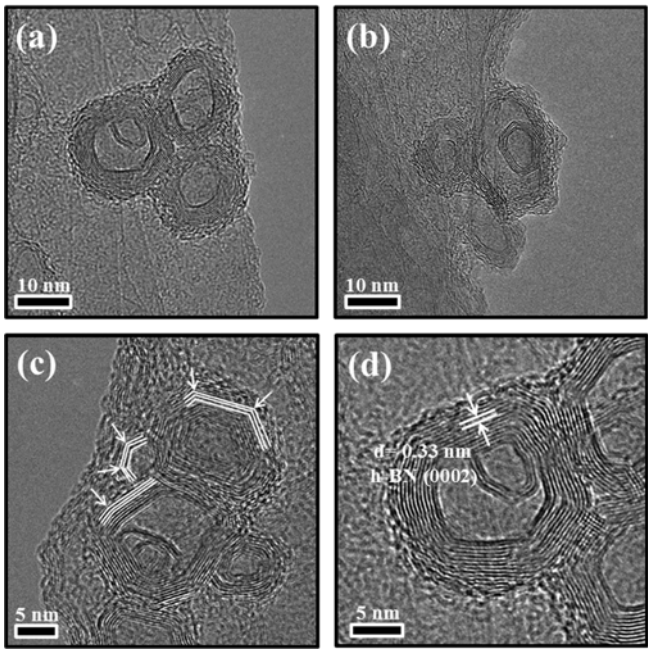

Fig. 1. (a,b,c) TEM images of typical *h*-BN fullerenes. In (c), we marked polyhedral shapes and corners. (d) Lattice-resolved TEM image of representative *h*-BN fullerenes.

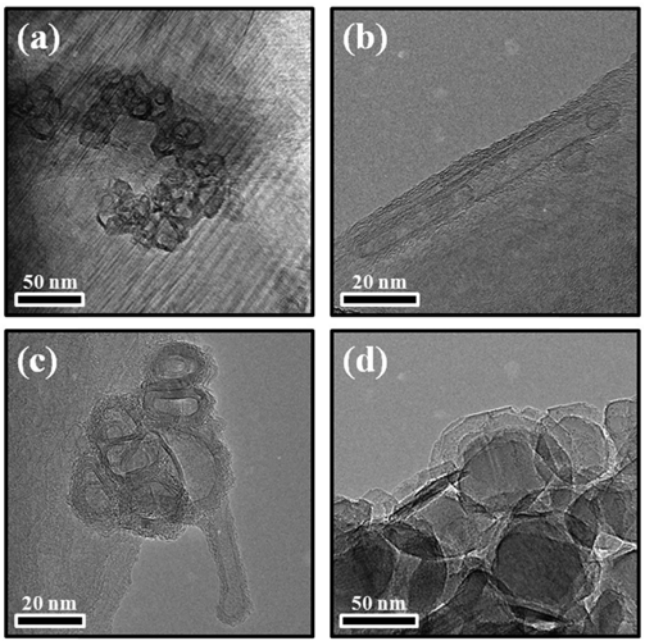

Fig. 2. TEM images of various *h*-BN fullerenes, which exhibit peculiar morphologies: (a) Several BN fullerenes are linked or connected. (b,c) BN nanotube-like structures and fullerenes are simultaneously observed. (d) TEM image of unzipped fullerenes.

tivity, and chemical inertness [19]. Furthermore, *h*-BN is very similar to graphene, because it has strong covalent sp^2 bonds in the plane, possessing the high in-plane mechanical strength and thermal conductivity [20]. Due to the graphene-like characteristics, the *h*-BN has found its use in protective coatings, deep ultraviolet emitter, charge leakage barrier layer, and transparent membrane [20]. Additionally, the *h*-BN can be used in ambient agitation energy harvesting, due to its giant flexoelectric effect [21]. Also, the *h*-BN can be used to fabricate the far-ultraviolet light-emitting devices [22].

Figures 2(a)-2(d) exhibit TEM images of fullerene-like nanostructures with an extraordinary morphology. In Fig. 2(a), several BN fullerenes were linked or connected. Such complicated structures have been theoretically predicted by computation [23]. Also, the formation of intermolecular bonds between BN fullerenes for stoichiometric and N-rich BN fullerenes has been scrutinized [24]. Figure 2(b) shows that fullerenes were captured within BN nanotubes. This observation indicates the co-existence of fullerene- and nanotube-like BN structures. In a previous study, the structure and formation of BN nanopeapods ($B_{12}N_{12}$ fullerenes in BN nanotubes) was simulated using the self-consistent density functional tight-binding method [25]. Similarly, Figure 2(c) indicates that BN nanotube-like structures formed near the BN fullerenes. Previous studies have reported the simultaneous formation of BN fullerenes and nanotubes [26]. BN fullerenes have been seen to coalesce and produce BN nanotubes [27]. Figure 2(d) shows peculiar structures similar to fullerenes. We

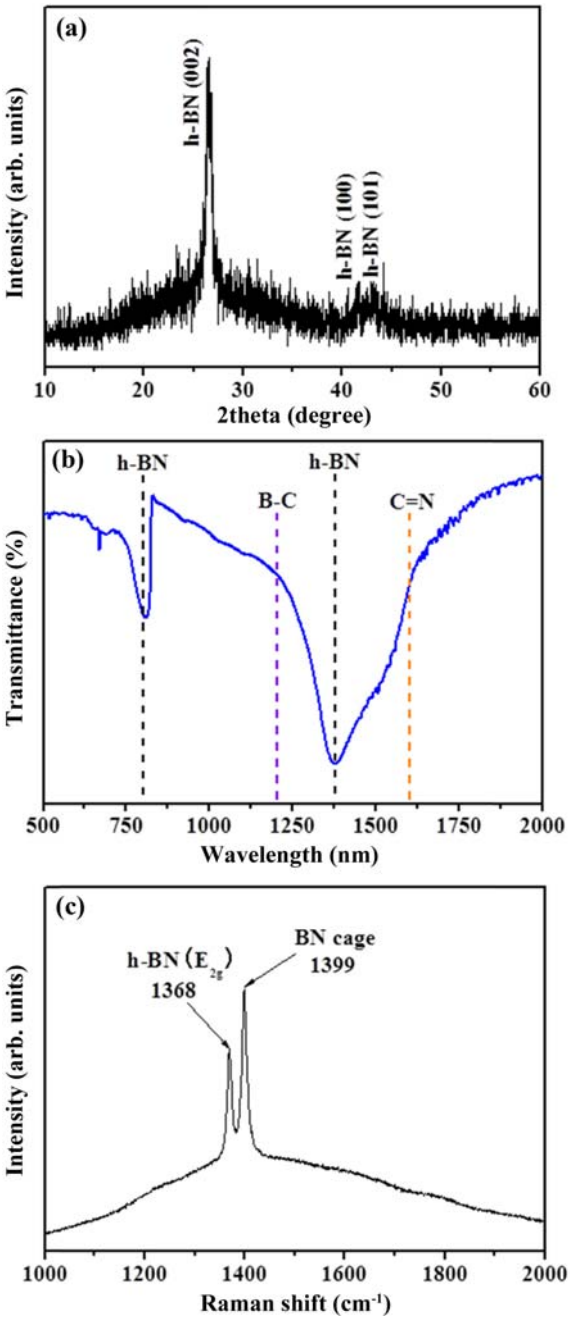

Fig. 3. (a) XRD pattern, (b) FTIR spectrum, and (c) Raman spectrum of the *h*-BN fullerenes.

surmise that the BN fullerenes unzipped and transformed into nanosheet-like structures. On the basis of Figs. 2(a) and 2(c), the average inner and outer diameters of BN fullerenes were in the ranges of 6-17 and 9-23 nm, respectively. In Figure 2(d), the average diameter of the sheet-like circular structures ranged from 39 to 52 nm. A simple calculation indicates that folding the circular sheet-like structures in Fig. 2(d) can create spheres with average diameters in the range of 13-17 nm, corroborating the assumption that BN fullerenes unzipped to

generate circular nanosheets.

Figure 3(a) shows an XRD spectrum of the as-synthesized product. The spectrum had a strong peak corresponding to the (002) diffraction of the *h*-BN phase (JCPDS card: No. 85-1068). In addition, weak peaks (or peak-like features) corresponded to the (100) and (101) diffractions of the *h*-BN phase.

The FTIR spectrum is shown in Fig. 3(b), showing clear absorption bands at approximately 800 and 1378 cm^{-1}, which are related to the *h*-BN structure. The band at 800 cm^{-1} can be assigned to out-of-plane bending of the sp^2 B-N-B bonds, whereas the band at 1378 cm^{-1} can be related to in-plane stretching of sp^2 B-N bonds [28]. The presence of carbon-rich B-C [29,30] and C=B bonds [29] is indicated by weak shoulders near 1200 and 1600 cm^{-1}, respectively, though they were present in small amounts.

In the Raman spectrum of the as-synthesized product (Fig. 3(c)), a sharp peak at approximately 1368 cm^{-1} was ascribed to the counter-phase B-N vibrational mode (E_{2g}) within the BN sheets [31]. This peak was ascribed to the first-order Raman effect of the *h*-BN structure [28,29]. The full-width-at-half minimum (FWHM) of the peak was 9.96 cm^{-1}. The nature of another strong peak around 1399 cm^{-1}, with a FWHM of 11.62 cm^{-1}, was not clear. However, Zope *et al*. previously reported a Raman active line (A_1) at 1395 cm^{-1} from $B_{36}N_{36}$ cages [30]. Thus, the line at 1399 cm^{-1} can reasonably be assigned to the Raman line from the *h*-BN fullerenes.

A PL spectrum of an as-synthesized sample measured at 8 K is presented in Fig. 4(a). To reveal the origin of the broad emission band, which could be a superimposition of several peaks, we used a deconvolution procedure based on Gaussian functions. The emission turned out to be composed of seven peaks centered at 1.92, 2.24, 2.41, 2.60, 2.82, 3.0, and 3.23 eV, respectively. The red emission band at 1.92 eV was previously observed in boron carbide nanowires and is related to the B_4C phase [32]. A small amount of B_4C phase was expected to exist in the *h*-BN fullerenes. The peak at 2.24 eV can be attributed to the B-O luminescence center [33]. A yellow-green emission, which is similar to the 2.41-eV peak in the present work, has been observed not only from BN whiskers [34], but also from BN nanoparticles [35]. A strong blue-green emission (2.60 eV) was found in room-temperature PL of BN whiskers [34] and bamboo-structured BN nanotubes [36]. Another possibility is that the 2.60-eV peak is a result of defects in the BCN phase [37]. The 2.82-eV peak (blue emission) was previously reported to be due to luminescence of BN whiskers [34], BN nanohorns [38], and BN nanotubes [39]. It was also ascribed to the B and N vacancies/defects [38] and bent BN layers/defects [39]. The blue-violet emission at 3.0 eV was reported in the cathodoluminescence spectrum of BN nanotubes [38]. For the 3.23 eV-peak, the ultraviolet emission was similar to that from *h*-BN or cylindrical BN nanotubes [39]. The above analyses

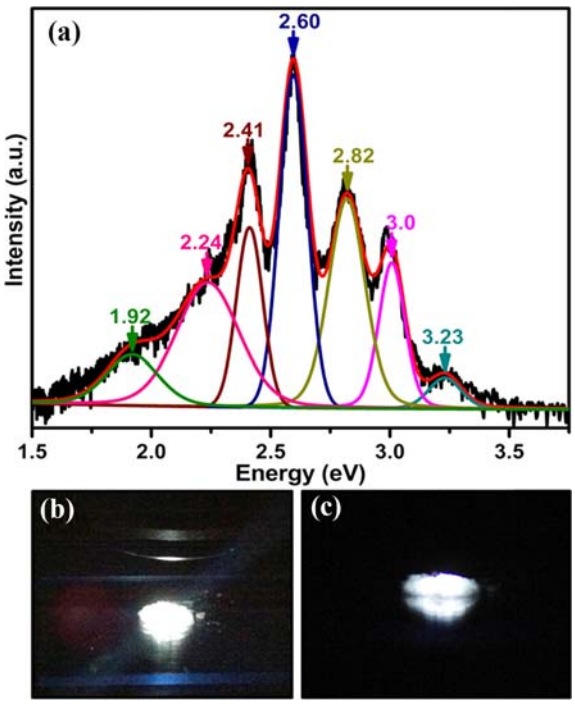

Fig. 4. (a) PL spectrum of the *h*-BN fullerenes. The spectrum was deconvoluted on the basis of Gaussian functions. (b) Side-view and (c) front-view dark-field PL image of the *h*-BN fullerenes.

indicate that most peaks in Fig. 4(a) are directly related to BN structures. Figs. 4(b) and 4(c) show the side-view and front-view, respectively, of dark-field PL images of the product. Photographs taken during the PL emission exhibit extraordinarily intense white-light emission. To our knowledge, there has been no report on the PL properties of BN fullerenes. Furthermore, the present PL is comprised of all range of visible lights, exhibiting an extremely bright white light. Accordingly, we compared the present PL to the emissions of similar structures, including BN whiskers, BN nanohorns, and BN nanotubes, etc.

We calculated chemical reactions in the GO, B_2O_3, C, and NH_3 systems using FactSage software [40]. On the basis of the literature on BN nanosheet growth [41], we propose a detailed formation mechanism of BN fullerenes (Fig. 5). Lin *et al*. reported that the lowest temperatures for incorporating BN into GO are 1500 °C and 900 °C, respectively, if N_2 and NH_3 are used as doping sources [41]. The associated reactions are as follows:

$$B_2O_3\ (gas) + 3C\ (sheets) + N_2\ (gas) = 2BN\ (sheets) + 3CO\ (gas). \quad (1)$$

$$B_2O_3\ (gas) + 3C\ (sheets) + 2\ NH_3\ (gas) = 2BN\ (sheets) + H_2O\ (gas) + H_2\ (gas) + CO\ (gas). \quad (2)$$

We tested these equations with FactSage:

1. At 900 °C:

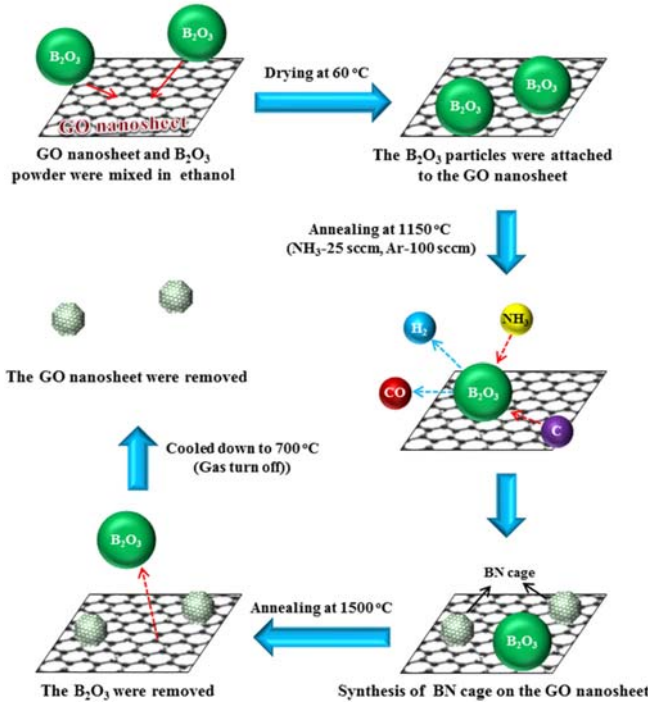

Fig. 5. Conceptual schematic of the growth of *h*-BN fullerenes by means of using the graphene oxide template.

B_2O_3 (gas) + 3C (sheets) + N_2 (gas) = 1.5 (gas) (50% CO, 50% N_2) + 0.744B_2O_3 + 2.238C + 0.512BN (3)

Only 0.256 (= 1-0.744) moles B_2O_3 were consumed to synthesize BN.

At 1243 °C:

B_2O_3 (gas) + 3C (sheets) + N_2 (gas) = 3CO (gas) + 2BN (4)

Therefore, thermodynamically, all B_2O_3 was consumed to synthesize BN at temperatures greater than 1243°C. The above reaction agrees with that of Han *et al*. [42].

2. At 900 °C:

B_2O_3 (gas) + 3C (sheets) + 2NH_3 (gas) = 4.96 (gas) (60% H_2, 30% CO, 10% N_2) + 1.5C + BN + 0.5B_2O_3 (5)

0.5 (= 1-0.5) moles of B_2O_3 were consumed to synthesize BN, which is approximately double the amount of B_2O_3 when using N_2 gas.

At 1150 °C:

B_2O_3 (gas) + 3C (sheets) + 2NH_3 (gas) = 6.00 (gas) (50% H_2, 50% CO) + 1.5 C + 2.00BN + 0.01B_2O_3 (6)

Almost all B_2O_3 was consumed to synthesize BN.

At 1500 °C:

B_2O_3 (gas) + 3C (sheets) + 2NH_3 (gas) = 6.00 (gas) (50% H_2, 50% CO) + 0.01C + 2.00BN (7)

All B_2O_3 was consumed to synthesize BN, and no H_2O was formed, as suggested by Lin *et al*. [41]. Therefore, the *h*-BN synthesis in this work can be described by the following scenario. GO and B_2O_3 powders were mixed and dried at 60 °C, allowing B_2O_3 to attach to the GO surface without any chemical reactions. The mixed power (GO + B_2O_3) was subsequently heated at 1150°C under a flow of a mixture of NH_3 and Ar gases. In this stage, B_2O_3 reacted with the NH_3 gas (*see* Eq. (6)), but no H_2O formed, as in Eq. (2), and almost all B_2O_3 was consumed to synthesize BN. By further increasing the temperature to 1500 °C, the little remaining B_2O_3 was fully consumed, leaving only BN on the GO surface. TEM-EDX investigation indicated that B_2O_3 was significantly removed (not shown here). During the subsequent cooling process, the residual GO was removed from the product.

Although considerable amount of studies on various nanostructures has been reported [43-45], the present work will be a cornerstone for the potential applications of nanostructures with novel materials and morphology.

4. CONCLUSIONS

We successfully fabricated *h*-BN fullerenes by heating a mixture of GO and B_2O_3 in the presence of NH_3 gas at 1150 °C. TEM images indicate that the product mainly contained BN fullerenes with a polyhedral morphology. Further TEM analysis revealed that the fullerene-like nanostructures had an extraordinary morphology. Lattice-resolved TEM images and XRD patterns indicated that the product mainly corresponded to the *h*-BN phase. In addition, FTIR and Raman spectra confirmed the formation of *h*-BN fullerenes. Dark-field PL images of the *h*-BN fullerenes showed conspicuously intense white-light emission. The growth model of the *h*-BN fullerenes was described based on thermodynamic calculations. The one-pot synthesis method developed in this work will be useful for practical applications of BN fullerenes in the future.

ACKNOWLEDGEMENTS

This work was supported by a National Research Foundation of Korea (NRF) grant funded by the Korean government (MEST) (No. NRF-2013R1A2A2A01068438).

REFERENCES

1. H. Kroto, J. Heath, S. O'Brien, R. Curl, and R. Smalley, *Nature* **318**, 162 (1985).
2. S. Alexandre, H. Chacham, and R. Nunes, *Phys. Rev. B* **63**, 045402 (2001).
3. S. Alexandre, M. Mazzoni, and H. Chacham, *Appl. Phys. Lett.* **75**, 61 (1999).

4. D. Golberg, Y. Bando, O. Stephan, and K. Kurashima, *Appl. Phys. Lett.* **73**, 2441 (1998).
5. N. Chopra, R. Luyken, K. Cherrey, V. Crespi, M. Cohen, S. Louie, and A. Zettl, *Science* **269**, 966 (1995).
6. T. Hirano, T. Oku, and K. Suganuma, *J. Mater. Chem.* **9**, 855 (1999).
7. I. Narita and T. Oku, *Diamond Relat. Mater.* **12**, 1146 (2003).
8. L. Rapoport, Y. Bilik, Y. Feldman, M. Homyonfer, S. Cohen, and R. Tenne, *Nature* **387**, 791 (1997).
9. J. Sloan, J. Cook, M. Green, J. Hutchison, and R. Tenne, *J. Mater. Chem.* **7**, 1089 (1997).
10. T. Oku and M. Kuno, *Diamond Relat. Mater.* **12**, 840 (2003).
11. L. Chkhartishvili, *Nano Studies* **2**, 139 (2010).
12. Q. Sun, Q. Wang, and P. Jena, *Nano Lett.* **5**, 1273 (2005).
13. T. Oku, T. Hirano, M. Kuno, T. Kusunose, K. Niihara, and K. Sudanuma, *Mater. Sci. Eng. B* **74**, 206 (2000).
14. O. Stephan, Y. Bando, A. Loiseau, F. Willaime, N. Shramchenko, T. Tamiya, and T. Sato, *Appl. Phys. A* **67**, 107 (1998).
15. L. Shi, Y. Gu, L. Chen, Y. Qian, Z. Yang, and J. Ma, *J. Sol. Stat. Chem.* **177**, 721 (2004).
16. W. Han, Y. Bando, K. Kurashima, and T. Sato, *Jpn. J. Appl. Phys.* **38**, L755 (1999).
17. F. Xu, Y. Xie, X. Zhang, S. Zhang, X. Liu, and X. Tian, *Inorg. Chem.* **43**, 822 (2004).
18. W. S. Hummers and R. E. Offerman, *J. Am. Chem. Soc.* **80**, 1339 (1958).
19. X. Ma, N. Lee, H. Oh, S. Ju ng, W. Lee, and S. Kim, *J. Cryst. Growth* **316**, 185 (2011).
20. K. K. Kim, A. Hsu, X. Jia, S. M. Kim, Y. Shi, M. Hofmann, D. Nezich, J. E. J. F. Rodriguez-Nieva, M. Dresselhaus, T. Palacios, and J. Kong, *Nano Lett.* **12**, 161 (2012).
21. I. Naumov, A. M. Bratkovsky, and V. Ranjan, *Phys. Rev. Lett.* **102**, 217601 (2009).
22. K. Watanabe, T. Taniguchi, T. Niiyama, K. Miya, and M. Taniguchi, *Nat. Photonics* **3**, 591 (2009).
23. V. Pokropivny, V. Skorokhod, G. Oleinik, A. Kurdyumov, T. Bartnitskaya, A. Pokropivny, A. Sisonyuk, and D. Sheichenko, *J. Sol. Stat. Chem.* **154**, 214 (2000).
24. V. Linss, S. Rodil, P. Reinke, M. Garnier, P. Oelhafen, U. Kreissig, and F. Richter, *Thin Solid Films* **467**, 76 (2004).
25. A. Enyashin and A. Ivanovskii, *Phys. Sol. Stat.* **50**, 390 (2008).
26. T. Hirano, T. Oku, and K. Suganuma, *Diam. Relat. Mater.* **9**, 625 (2000).
27. Y. Yong, K. Liu, B. Song, P. He, P. Wang, and H. Li, *Phys. Lett. A* **376**, 1465 (2012).
28. R. Geick, C. Perry, and G. Rupprecht, *Phys. Rev.* **146**, 543 (1966).
29. M. Mannan, M. Nagano, K. Shigezumi, T. Kida, N. Hirao, and Y. Baba, *Am. J. Applied Sci.* **5**, 736 (2007).
30. R. Gago, I. Jimenez, F. Agullo-Rueda, J. Albella, Z. Czigany, and L. Hultman, *J. Appl. Phys.* **92**, 5177 (2002).
31. J. Wu, W. Han, W. Walukiewicz, J. Ager III, W. Shan, E. Haller, and A. Zettl, *Nano Lett.* **4**, 647 (2004).
32. L. Bao, C. Li, Y. Tian, J. Tian, C. Hui, X. Wang, C. Shen, and H. Gao, *Chin. Phys. B* **17**, 4585 (2008).
33. C. Tang, Y. Bando, C. Zhi, and D. Golberg, *Chem. Commun.* **44**, 4599 (2007).
34. B. Zhong, X. Huang, G. Wen, L. Xia, H. Yu, and H. Bai, *J. Phys. Chem. C* **114**, 21165 (2010).
35. X. Li, C. Shao, S. Qiu, F. Xiao, W. Zheng, and O. Terasaki, *Mater. Lett.* **44**, 341 (2000).
36. Z. Chen, J. Zou, G. Liu, F. Li, H. Cheng, T. Sekiguchi, M. Gu, X. Yao, L. Wang, and G. Lu, *Appl. Phys. Lett.* **94**, 023105 (2009).
37. X. Bai, E. Wang, J. Yu, and H. Yang, *Appl. Phys. Lett.* **77**, 67 (2000).
38. C. Zhi, Y. Bando, C. Tang, and D. Golberg, *Appl. Phys. Lett.* **87**, 063107 (2005).
39. H. Chen, Y. Chen, C. Li, H. Zhang, J. Williams, Y. Liu, Z. Liu, and S. Ringer, *Adv. Mater.* **19**, 1845 (2007).
40. C. W. Bale, E. Belisle, P. Chartrand, S. A. Decterov, G. Eriksson, K. Hack, I. H. Jung, Y. B. Kang, J. Melancon, A. D. Pelton, C. Robelin, and S. Peterson, *CALPHAD* **33**, 295 (2009).
41. T. W. Lin, C. Y. Su, X. Q. Zhang, W. Zhang, Y. H. Lee, C. W. Chu, H. Y. Lin, M. T. Chang, F. R. Chen, and L. J. Li, *Small* **8**, 1384 (2012).
42. W. Q. Han, R. Brutchey, T. D. Tilley, and A. Zettl, *Nano Lett.* **4**, 173 (2004).
43. S. J. Yoo and W. J. Kim, *Korean J. Met. Mater.* **52**, 561 (2014).
44. C.-H. Lim, H.-S. Kim, Y.-T. Yu, and J.-S. Park, *Met. Mater. Int.* **20**, 323 (2014).
45. H. Ghasemi-Nanesa, M. Nili-Ahmadabadi, A. Mirsepasi, and C. Zamani, *Met. Mater. Int*. **20**, 201 (2014).